

# Analytical Methods

Accepted Manuscript



This is an *Accepted Manuscript*, which has been through the Royal Society of Chemistry peer review process and has been accepted for publication.

*Accepted Manuscripts* are published online shortly after acceptance, before technical editing, formatting and proof reading. Using this free service, authors can make their results available to the community, in citable form, before we publish the edited article. We will replace this *Accepted Manuscript* with the edited and formatted *Advance Article* as soon as it is available.

You can find more information about *Accepted Manuscripts* in the [Information for Authors](#).

Please note that technical editing may introduce minor changes to the text and/or graphics, which may alter content. The journal's standard [Terms & Conditions](#) and the [Ethical guidelines](#) still apply. In no event shall the Royal Society of Chemistry be held responsible for any errors or omissions in this *Accepted Manuscript* or any consequences arising from the use of any information it contains.

1  
2  
3 1 **Green synthesis and evaluation of isoquercitrin imprinted polymers**  
4  
5 2 **for class-selective separation and purification of flavonol glycosides**  
6  
7  
8  
9 3

10 4 Xiang-Jie Li<sup>a,b</sup> Xiu-Xiu Chen<sup>a,b</sup> Guan-Yin Sun<sup>a,b</sup> Yong Xin Zhao<sup>a,b</sup>

11  
12  
13 5 Zhao-Sheng Liu<sup>a,b\*</sup> Haji Akber Aisa<sup>\*, a,b</sup>  
14  
15 6

16  
17 <sup>a</sup>*Xinjiang Technical Institute of Physics and Chemistry, Chinese Academy of Sciences,*  
18 *Urumqi 830011, Xinjiang, China*

19 <sup>b</sup>*State Key Laboratory Basis of Xinjiang Indigenous Medicinal Plants*  
20 *Resource Utilization, Xinjiang Technical Institute of Physics and Chemistry,*  
21 *Chinese Academy of Sciences, Urumqi 830011, China*  
22  
23  
24  
25  
26

27 14 Correspondence: Dr. Zhao-Sheng Liu, Xinjiang Technical Institute of Physics and  
28  
29  
30 15 Chemistry, Chinese Academy of Sciences, Urumqi 830011, Xinjiang, China  
31  
32

33 16 **E-mail:** zhaoshengliu@sohu.com  
34  
35

36 17 **Fax:** +86-22-23536746  
37  
38

39 18 Correspondence: Haji Akber Aisa, Xinjiang Technical Institute of Physics and  
40  
41  
42 19 Chemistry, Chinese Academy of Sciences, Urumqi 830011, Xinjiang, China  
43  
44

45 20 E-mail: haji@ms.xjb.ac.cn  
46  
47

48 21  
49  
50 22 **Keyword:** Monolithic column; molecularly imprinted polymer; isoquercitrin; solid  
51  
52  
53 23 phase extraction; enrichment; HPLC  
54  
55  
56  
57  
58  
59  
60

1  
2  
3 254  
5 26**Abstract**6  
7 27

8  
9  
10 28 A method of solid-phase extraction (SPE) against isoquercitrin (ISO) from  
11  
12 29 natural plant extracts was proposed based on molecularly imprinted polymers (MIPs).  
13  
14  
15 30 The efforts in the present work aim at the emphasis on the topic of “green” chemistry,  
16  
17  
18 31 i.e., the use of green solvent, ionic liquid with a high percentage (63.2%-69.3%) in the  
19  
20  
21 32 total volume of porogenic solvent. For the preparation of ISO-MIPs monolith,  
22  
23 33 4-vinylpyridine was used as the functional monomer, and ethylene glycol  
24  
25 34 dimethacrylate was the cross-linking monomer, using a mixture of  
26  
27  
28 35 1-butyl-3-methylimidazoliumtetrafluoroborate (ionic liquid)-N’N-dimethylformamide  
29  
30  
31 36 (DMF)-dimethyl sulfoxide as porogen. It was found that the type of functional  
32  
33 37 monomer, the ratio of template to functional monomer, crosslinking degree, and level  
34  
35 38 of DMF, and the composition of mobile phase greatly affected the retention of the  
36  
37  
38 39 template and performance of molecular recognition. The optimal MIPs were used as  
39  
40  
41 40 solid-phase extraction (SPE) sorbents for purification of ISO, hyperoside, and  
42  
43  
44 41 astragalins and a SPE protocol was optimised for the type of loading solvent, amount  
45  
46 42 of MIPs, washing and elution solvent. It was found that the most suitable solvents for  
47  
48  
49 43 loading, washing and elution step were methanol-water (70:30, v/v), methanol-water  
50  
51 44 (20:80, v/v) and acetonitrile-water (30:70, v/v), respectively. The highest recovery  
52  
53 45 rate of ISO, hyperoside, and astragalins was 87.78%, 93.26% and 83.25%, respectively,  
54  
55  
56 46 from the crude extract of cotton flower.

57  
58 47  
59  
60

## 48 1. Introduction

49 Flavonoids are phenolic substances found widely in nature with a range of  
50 biological and pharmacological activities.<sup>1-3</sup> Both the flavonoids and their metabolites  
51 have display an in vivo antioxidant activity, which is due to their ability to reduce free  
52 radical formation and to scavenge free radicals. Therefore, the capacity of flavonoids  
53 to act as antioxidants in vitro has been the subject of studies in the past years, and the  
54 important structure–activity relationships of the antioxidant activity have been  
55 established. Up to date, the antioxidant efficacy in vivo of flavonoids has been less  
56 thoroughly documented, possibly due to the limited knowledge on their  
57 pharmacokinetics derived from the lack of highly pure flavonoids.

58 Isoquercitrin (Quercetin-3-O-glucoside) (ISO) and its analogues (Fig. 1),  
59 hyperoside, and astragalin are the important flavonoids found in flowers of  
60 *Gossypium herbaceum* L. and leaves of *Apocynum lancifolium* Rus. and related  
61 species. Because of the complexity of the sample matrix, ISO and its analogues need  
62 to be separated from interference prior to analysis and a number of analytical  
63 techniques have been developed.<sup>4-7</sup> Among them, high-performance liquid  
64 chromatography (HPLC) is commonly used<sup>8-12</sup> and pretreatment steps before  
65 chromatographic analysis are often required for extracting as well as cleaning up the  
66 target analytes from sample. However, to achieve highly pure flavonoids from  
67 vascular plants is difficult because they occur in very low amounts in plant with very  
68 rich in interfering substances.

69 Solid-phase extraction (SPE) is one of the most convenient and high performance

1  
2  
3  
4 70 technologies for separation of bioactive compounds from plants.<sup>13</sup> It can help  
5  
6 71 minimize the use of organic solvents which are regulated as priority pollutants. A  
7  
8 72 number of sorbents, e.g., C<sub>18</sub>, spherical silica, alumina, and carbon material, have  
9  
10 73 been used in SPE in previous reports. However, all of the techniques present some  
11  
12 74 disadvantages as the co-extraction of interfering compounds with a similar polarity to  
13  
14 75 the analytes, which hamper in the subsequent determination of the compounds of  
15  
16 76 interest due to absence of selectivity of absorption fillers.

17  
18  
19  
20  
21 77 Recently, molecularly imprinted polymers (MIPs) have emerged as powerful  
22  
23 78 sorbent for the selective solid-phase extraction of single compounds or compound  
24  
25 79 classes from complex matrices.<sup>14-16</sup> These highly cross-linked polymers display  
26  
27 80 binding sites in cavities creating the complementary domains of the given molecule  
28  
29 81 with good physicochemical stability, practicality, and predetermination selectivity to  
30  
31 82 the template molecule as well as to the structural analogues. In recent years, attempts  
32  
33 83 have been made to apply MIPs to SPE with special recognition ability to replace  
34  
35 84 conventional sample pretreatment materials. Advantages of the MIPs solid phase  
36  
37 85 extraction (MISPE) are not only in terms of preconcentration and cleaning of samples,  
38  
39 86 but also selective extraction of target analytes, low cost relatively, good mechanical  
40  
41 87 properties and long life, which is particularly important in complex or highly  
42  
43 88 contaminated samples.

44  
45  
46  
47  
48  
49  
50  
51 89 Over the past decade there has been an increased emphasis on the topic of  
52  
53 90 “green” chemistry and chemical processes. These efforts aim at the total elimination  
54  
55 91 or at least the minimization of generated waste and the implementation of sustainable  
56  
57  
58  
59  
60

1  
2  
3  
4 92 processes. Any attempt at meeting these goals must comprehensively address these  
5  
6 93 principles in the design of a synthetic route or preparation approach. Utilization of  
7  
8  
9 94 nontoxic chemicals, environmentally benign solvents, and renewable materials are  
10  
11 95 some of the key issues that merit important consideration in a green synthetic strategy.  
12  
13 96 For flavonoids, a number of paper related to flavonoids-MIP have been published,<sup>17-21</sup>  
14  
15  
16 97 but volatile solvent, e.g., organic small molecules, had to be used as porogenic solvent,  
17  
18  
19 98 which does not meet the requirements of the green chemistry.

20  
21 99 In view of facts above, we intend to propose a greener approach for the synthesis  
22  
23  
24 100 of imprinted polymer for flavonoids. For this purpose, a green and non-volatile  
25  
26 101 solvent, ionic liquid (IL), was used as porogenic solvent to prepare MIP. As a unique,  
27  
28  
29 102 environmentally friendly solvent of low vapor pressure with excellent solvation  
30  
31 103 qualities and chemical/thermal stability, IL has been used in precipitation  
32  
33 104 polymerization to form MIP nano- or micro-particles,<sup>22,23</sup> as well as MIP  
34  
35  
36 105 monolith.<sup>24-26</sup> However, the use of IL to prepare MIP is still limited and the design of  
37  
38  
39 106 IL-based MIP is challenge because of its polar nature affecting the formation of  
40  
41 107 complexes in traditional non-covalent imprinting method. In the present study, ISO  
42  
43  
44 108 was chosen as template, 4-VP as monomer, EDMA as crosslinker, and a ternary,  
45  
46 109 non-volatile solvent mixture, i.e., IL/DMSO/DMF as porogens to prepare MIP for  
47  
48  
49 110 class-selective separation and purification of flavonol glycosides. The effect of  
50  
51 111 polymerization parameters on the selectivity and affinity of the resultant imprinted  
52  
53  
54 112 polymers was investigated. By our knowledge, this is the first report of the  
55  
56  
57 113 preparation of MIP against ISO.  
58  
59  
60

## 114 2 Experimental

### 115 2.1 Materials

116 Isoquercitrin (ISO, 98%), hyperoside (HYP, 98%), catechin (C, 98%) and astragaloside  
117 (AST, 98%) were purchased from Shifeng Biotechnology Co., Ltd. (Shanghai, China).  
118 Ethyleneglycol dimethacrylate (EDMA, 98%) and 4-vinylpyridine (4-VP, 98%) were  
119 purchased from Sigma (St. Louis, MO, USA). N,N-Dimethylformamide (DMF, 99.6%)  
120 and 1-butyl-3-methylimidazoliumtetrafluoroborate ([BMIM]BF<sub>4</sub>, AR) were purchased  
121 from Jiecheng Chemical Co., Ltd (Shanghai, China). Methyl gallate (MG, 98%) were  
122 purchased from Hongsheng Co., Ltd. (Beijing, China). Gallic acid (GA, 98%) was  
123 purchased from Guangtuo Chemical Co., Ltd. (Beijing, China). m-Hydroxybenzoic  
124 (MHBA, 98%) acid was purchased from Baishun chemical Co., Ltd. (Beijing, China).  
125 p-hydroxybenzoic (PHBA, 98%) and azobisisobutyronitrile (AIBN, AR) were purchased  
126 from Kemiou Chemical Reagent Co., Ltd. (Tianjin, China). Dimethyl sulfoxide (DMSO,  
127 HPLC grade) was purchased from Tianjin Jiangtian Pharmachem Technology Co., Ltd.  
128 (Tianjin, China). Acrylamide (AM, 98%) was purchased from Tianjin Bodi Pharmachem  
129 Co., Ltd. (Tianjin, China). Other reagents were HPLC grade. The crude extract from  
130 cotton flower was obtained from Xinjiang Technical Institute of Physics and Chemistry.

### 131 2.2 Instrumentation

132 The HPLC system K3800 consisting of UV2000/2000D UV/Vis detector, P2000  
133 high-pressure pump, K3800 chromatography workstation (Kai'ao Technology  
134 Development Co. Ltd., Beijing, China) was used. The detection was performed at 254  
135 nm with a flow rate of 0.5 mL/min. All of mobile phases were filtered through a 0.22

1  
2  
3  
4 136  $\mu\text{m}$  membrane from Millipore before use. Column void volumes were measured by  
5  
6 137 injection of 20  $\mu\text{L}$  of acetone (0.1%, v/v) in the corresponding mobile phase.  
7

8  
9 138 The retention factor,  $k'$ , is calculated by:<sup>24</sup>

10  
11 139 
$$k' = \frac{(t_R - t_0)}{t_0} \quad (1)$$
  
12

13  
14 140 where  $t_R$  is the retention time of retained peak,  $t_0$  is the retention time of unretained  
15  
16 141 acetone.  
17

18  
19 142 Imprinting factor (IF) is calculated by the equation:<sup>24</sup>

20  
21 143 
$$\text{IF} = k'_{\text{MIP}} / k'_{\text{NIP}} \quad (2)$$
  
22

23  
24 144 where  $k'_{\text{MIP}}$  is the retention factor of the template molecule eluted from the imprinted  
25  
26 145 polymer and  $k'_{\text{NIP}}$  is the retention factor of the template molecule eluted from the  
27  
28 146 non-imprinted polymer.  
29

### 30 31 147 **2.3 Preparation of ISO-imprinted monoliths**

32  
33  
34 148 Imprinted monoliths were prepared by following process: the pre-polymerization  
35  
36 149 mixture was obtained by mixing ISO, 4-VP, EDMA, AIBN (20 mg), and a mixture of  
37  
38 150 [BMIM]BF<sub>4</sub>/DMF/DMSO, as show in Table 1. Then the mixture was sonicated for 20  
39  
40 151 minutes and injected into stainless steel column (100 mm×4.6 mm). The column was  
41  
42 152 then sealed and submerged in 60 $\square$  water bath for 18 h. After completion of the  
43  
44 153 polymerization, the unreacted reagents were rinsed with acetonitrile. Then the  
45  
46 154 template molecules were removed with methanol/acetic acid (9:1). Blank monolith  
47  
48  
49  
50  
51 155 was prepared in same way without imprinted molecules.  
52

### 53 54 156 **2.4 Scanning electron microscopy**

55  
56 157 Scanning electron microscopy (SEM) was used for the characterization of the  
57  
58  
59  
60

1  
2  
3  
4 158 monoliths. Samples were sputter-coated with gold before obtaining images. All  
5  
6 159 scanning electron micrographic images were obtained by using a Shimadzu SS-550  
7  
8  
9 160 scanning electron microscope, operated at 15 kV and a filament current of 60 mA.

## 11 161 **2.5 Mercury porosimetry**

12  
13  
14 162 Mercury intrusion and extrusion experiments on the monolithic polymer samples  
15  
16 163 were performed over a wide range for pressures starting in vacuum up to 60,000 psi (1  
17  
18 164 psi =  $6.895 \times 10^{-3}$  MPa) by a poremaster 60 instrument (Quantachrome Instruments,  
19  
20  
21 165 Boyton Beach, FL, USA). Data acquisition was performed in autospeed continuous  
22  
23 166 scanning mode enabling maximum resolution speed in the absence of intrusion or  
24  
25  
26 167 extrusion and maximum resolution and sufficient equilibration time (sampling time)  
27  
28  
29 168 when intrusion or extrusion was occurring rapidly with changing pressure.

## 31 169 **2.6 Separation and purification of isoquercitrin from crude extract of cotton** 32 33 34 170 **flower**

35  
36 171 The resulting MIPs were pumped out from the stainless steel column and ground  
37  
38 172 and sieved with 71  $\mu$ m-sieve. Then 0.9 g of uniform granule was packed into a  
39  
40  
41 173 home-made SPE column (200 mm $\times$ 9 mm) with a small piece of cotton placed at the  
42  
43  
44 174 end of the column. The crude extract (10.09 mg) was resolved by 0.5 ml of methanol  
45  
46 175 aqueous solution (70%, v/v) and loaded on the MISPE column, which was activated  
47  
48  
49 176 with 10 ml methanol before. The sample of the crude extract was washed and eluted,  
50  
51  
52 177 to separate ISO and its analogues from interferences. All significant variables were  
53  
54 178 investigated. As show in Table S1, the optimum SPE protocol was made according to  
55  
56 179 the following steps: the column was rinsed by methanol/water (20:80)(5 ml) and  
57  
58  
59  
60

1  
2  
3  
4 180 methanol/water (25:75)(5 ml), respectively. Acetonitrile-water mixture (30:70) was  
5  
6 181 percolated through the MIP cartridge to obtain isoquercitrin and structural analogues  
7  
8  
9 182 and segmented collecting by TLC. The target substance was found in the eluted  
10  
11 183 solution with flushing volume of 3-7 ml. The content of ISO and its analogues in  
12  
13 184 purified sample and crude extract were determined by HPLC. As a reference, the  
14  
15 185 solution of crude extract was analyzed directly on a C18 column.

16  
17  
18 186 The HPLC system consisting of a quaternary gradient LPG-3400SD pump, a  
19  
20 187 VWD-3100 detector (including flow cell), WPS-3000SL auto sampler, online  
21  
22 188 degasser and reagent rack and four bottles (Thermofisher, USA) was used. Separation  
23  
24 189 was performed on Sun Fire TM C18 (250 mm×4.6 mm, 5 μm) (Waters).

### 25 26 27 28 29 190 **3. Results and discussion**

#### 30 31 191 **3.1 Preparation of ISO-imprinted monolithic column**

##### 32 33 192 **3.1.1 Choice of functional monomer**

34  
35  
36  
37 193 In general, the relatively strong interactions involved between functional  
38  
39 194 monomers and the template often lead to the imprinted polymer with higher affinity.  
40  
41 195 Since methacrylic acid (MAA) is the most commonly employed functional monomer  
42  
43 196 for non-covalent imprinting, the starting point for the optimization was the previously  
44  
45 197 reported MIP of the poly(MAA-co-EDMA)-type targeted toward ISO, but the column  
46  
47 198 pressure was too high when the ratio of template to monomer was 1:4. We also used  
48  
49 199 non-covalent neutral monomer acrylamide (AM) and to prepare MIP as it forms  
50  
51 200 stronger hydrogen-bonds in polar protic solvent than MAA. In present work, it was  
52  
53 201 found that 4-VP other than MAA or AA (IF < 1) was the optimal monomer, which  
54  
55  
56  
57  
58  
59  
60

1  
2  
3  
4 202 may be due to potential complexation through hydrogen bonding of the free hydroxyl  
5  
6 203 groups and the nitrogens of the pyrazine cycle (Fig. 1a). HPLC was used to evaluate  
7  
8  
9 204 the performance of ISO-MIP monolith with a mobile phase of methanol/water/acetate  
10  
11 205 acid (90/9/1, v/v/v), in which water was added to reduce non-specific interactions.  
12  
13

### 14 206 **3.1.2 Optimization of ratio of template to functional monomer**

15  
16  
17 207 The influence of template-monomer (T/M) molar ratio on the imprinting factor  
18  
19  
20 208 of the resultant MIP monoliths was studied because the molar relationship between  
21  
22  
23 209 the monomer and template has been found to be important with respect to the number  
24  
25 210 and quality of recognition sites in MIPs.<sup>28</sup> In this work, we varied the molar ratio of  
26  
27  
28 211 template to monomer by setting the ratio of 4-VP to EDMA of 1:5, a ratio of classic  
29  
30 212 functional monomer to crosslinker as the starting point of the study. As shown in Fig.  
31  
32  
33 213 S1a, the imprinting factors of the resulting MIPs increase with the increased  
34  
35 214 concentration of the monomer. Obviously, the result may be due to more imprinting  
36  
37  
38 215 sites as the increase in the amount of the monomer. However, further increase in the  
39  
40 216 molar ratio of template to monomer led to MIPs monolith with high back pressure and  
41  
42  
43 217 further evaluation was impossible. The best imprinting factor (>2.5) was obtained on  
44  
45 218 P3, which was prepared with a T/M ratio of 1:5.

### 46 47 219 **3.1.3 Optimization of ratio of functional monomer to crosslinker**

48  
49  
50 220 The effects of cross-linking monomer on the retention factors and imprinting  
51  
52  
53 221 effect of the resulting MIP monoliths were also investigated (Fig. S1b). We have  
54  
55 222 prepared 4-VP/EDMA-polymers having a functional monomer/crosslinker (M:C)  
56  
57  
58 223 ratio of 1: 5, which contained varying ratio of M:C (1:3, 1:4 and 1:5). It was found  
59  
60

224 that the optimum ratio of 4-VP to EDMA was 1:4 in terms of imprinting factor ( $>1.7$ ).

225 In general, high levels of cross-linking agent are used, the imprinting sites retain their

226 shape quite well after removal of the templates. However, the result suggested that

227 high levels of crosslinker might lead to the stiffness of the polymer network increased

228 severely, thus decrease the accessibility of the cavities significantly.<sup>29</sup> As a result, a

229 compromise must be found between an inflexible arrangement of the polymer chains

230 to give high selectivity and an appropriate degree of flexibility, which is necessary for

231 good accessibility of the cavities and rapid attainment of binding equilibrium.

### 232 3.1.4 Effect of DMF ratio

233 Previously, a mixture of DMF-DMSO-[BMIM]BF<sub>4</sub> has been used as porogen to

234 synthesize MIP monolith for polar template.<sup>24</sup> [BMIM][BF<sub>4</sub>] was found to be the

235 unique porogen to achieve the MIP monolith with desired chromatographic behaviors,

236 which might be attributed to low degree of polymer swelling in ionic liquid.<sup>22,23</sup> At

237 present investigation, it was found that DMF-DMSO-[BMIM]BF<sub>4</sub> also fitted to

238 prepare ISO-MIP monolith. DMSO was used as a solvent to dissolve adequate amount

239 of ISO, and the minimum amount of DMSO was used to minimize the interference of

240 the electrostatic interactions most commonly utilized between the functional

241 monomers and the template. Thus, the effect of the composition of porogenic solvent

242 on the performance of ISO-MIP monolith was studied with by shifting the amount of

243 DMF in the pre-polymerization mixture (Fig. S1c). It was found that when the

244 percentage of DMF was beyond 8.8%, there was no imprinting effect on the resulting

245 MIP monolith at all. With the decrease in the ratio of DMF in the porogenic solvent,

1  
2  
3  
4 246 both capacity factor and imprinting factor of the template increased. However, further  
5  
6 247 decrease in the content of DMF leads to peak split of the template on the resultant  
7  
8  
9 248 MIP monolith. In this work, the optimum content of DMF was 2.2% (v/v) in terms of  
10  
11 249 imprinting factor. It should be noted that both DMF and DMSO used in the  
12  
13  
14 250 preparation of MIP monolith are non-volatile solvent with high boiling point.  
15

### 16 251 **3.2 Morphological characterization of MIP monolith**

17  
18  
19 252 The morphology of the ISO-based MIP (P15) was observed by SEM. As shown  
20  
21 253 in Fig. 2a, the MIP monolith shows an agglomerate of microspheres with a  
22  
23  
24 254 cauliflower form that are fused into a continuous structure. In addition, remarkable  
25  
26 255 macropores could be found in the polymer skeleton, allowing low backpressure even  
27  
28  
29 256 at high flow rate. This macroporous structure is related to green solvent [BMIM]BF<sub>4</sub>  
30  
31 257 used for polymerization. Indeed, ionic liquid generally lead to macroporous structure  
32  
33  
34 258 and lower capacity than apolar solvents.<sup>24,25</sup>  
35

36  
37 259 The pore size distribution of the optimal MIP monolith P15 was been further  
38  
39 260 studied with mercury intrusion porosimetry (Fig. 2b). The mode pore size of the MIP  
40  
41 261 monolith, i.e., the pore diameter at the maximum of the pore distribution curve, was  
42  
43  
44 262 1.3  $\mu\text{m}$ , suggesting larger superpores. The result was in agreement with SEM very  
45  
46 263 well.  
47

### 48 264 **3.3 Thermodynamic study**

49  
50  
51 265 The impact of temperature on the retention of ISO was investigated by shifting  
52  
53  
54 266 temperature from 25°C to 45°C on the MIP column (P15). With increasing column  
55  
56 267 temperature, it was observed that the retention factors of solutes declined. Data  
57  
58  
59  
60

1  
2  
3  
4 268 obtained from the thermodynamic properties of the separation was evaluated by van't  
5  
6 269 Hoff equation:<sup>24</sup>

7  
8  
9 270 
$$\ln k' = -\frac{\Delta H}{RT} + \frac{\Delta S}{R} + \ln \Phi \quad (3)$$

10  
11  
12  
13 271 
$$\ln \alpha = -\frac{\Delta \Delta H}{RT} + \frac{\Delta \Delta S}{R} \quad (4)$$

14  
15  
16 272  $\Delta H$ ,  $\Delta S$ ,  $\Delta \Delta H$ , and  $\Delta \Delta S$  can be obtained from the slopes and intercepts of linear  
17  
18  
19 273 portion of the relative equations (3) and (4).

20  
21 274 Over the temperature range in our experiment, the van't Hoff plots were linear  
22  
23  
24 275 for the analogues of ISO on the MIP monolith (P15)(Fig. 3). As shown in Table 2, the  
25  
26 276 absolute values of  $\Delta H$  for ISO were larger than the analogues. This suggested that ISO  
27  
28  
29 277 has stronger affinity to the recognition sites, and could form a more stable complex  
30  
31  
32 278 than the analogues during their matching in the micro-cavities on the MIP. Moreover,  
33  
34 279 the fact that  $|\Delta \Delta H| > T|\Delta \Delta S|$  indicated that the separation between two analogues on  
35  
36 280 this monolithic MIPs was an enthalpy-controlled process.<sup>24,29</sup>

37  
38  
39 281 As shown in Table 2, a value of negative enthalpy suggests interactions between  
40  
41 282 the template and the polymer of hydrogen-bonding, ion-pairing, or van der Waals  
42  
43  
44 283 interactions. The negative entropy indicates an increase in the order of the  
45  
46 284 chromatographic system as the solute was bound by the polymer, which is a result of  
47  
48  
49 285 an energetic penalty the freezing of a rotor Gibbs free energy change.<sup>30</sup> The absolute  
50  
51 286 value of  $T\Delta S = 3.40-3.68 \text{ kcal mol}^{-1}$  ( $14.2-15.4 \text{ kJ mol}^{-1}$ ) is ca. three times higher than  
52  
53  
54 287 the value  $T\Delta S = 1-1.4 \text{ kcal mol}^{-1}$  per rotor calculated for weak complex. Assuming  
55  
56 288 that at 323 K the binding sites have an open conformation and desolvation effects are  
57  
58  
59  
60

1  
2  
3  
4 289 minimal, it is possible to conclude that only a small part of the template molecule is  
5  
6 290 embedded into the binding cavity; otherwise, the energetic penalty will be large.  
7  
8

### 9 291 **3.4 Separation and enrichment of ISO and its analogues by MISPE.**

#### 10 292 **3.4.1. Selectivity of ISO MIP**

11  
12  
13  
14 293 To further evaluate the selectivity of ISO-imprinted polymer, the retention of  
15  
16 294 analogues of ISO, hyperoside, astragalin, C, GA, MG, MHBA, PHBA, has been  
17  
18  
19 295 tested by HPLC in same chromatographic conditions above. As shown in Fig. 5, it  
20  
21 296 indicated that the imprinted molecule was much stronger bonding with specific site  
22  
23  
24 297 than other compounds tested. The IF value of hyperoside, astragalin, quercetin, C, GA,  
25  
26 298 MG, MHBA and PHBA, was 2.16, 1.43, 2.02, respectively. The results indicated  
27  
28  
29 299 that the more great extent of similarity to ISO, the more close value of retention factor  
30  
31 300 of analogues to ISO. Furthermore, the retention time of quercetin on the  
32  
33  
34 301 MIP-monolith was much longer than ISO and its analogues, which may be due to the  
35  
36 302 greater nonpolar nature of quercetin in addition to similar groups to ISO. Thus, the  
37  
38  
39 303 MIP monolith has revealed the potential property for separating ISO and its analogues  
40  
41 304 from crude extracts of plants.  
42  
43

#### 44 305 **3.4.2. Selection of loading solvent**

45  
46 306 In general, the loading solvent should not rinse the template molecules from MIP  
47  
48  
49 307 in addition to the ability to dissolve ISO. A number of solvents or solvents mixture,  
50  
51 308 such as methanol, acetonitrile, and methanol-water (90:10, 70:30 and 50:50, v/v),  
52  
53  
54 309 were used to perform scouting experiments. Acetone failed to be as loading solvent  
55  
56 310 due to the low solubility of ISO in it. Keeping the amount of ISO (2 mg) and MIPs  
57  
58  
59  
60

1  
2  
3  
4 311 (0.9 g) as constant, the volume of different kind of loading solvent was increased from  
5  
6 312 2 to 6 ml and the percentage of retention in the volume-point of various loading  
7  
8 313 solvent was measured. In our work, methanol-water (70:30, v/v) was chosen as  
9  
10 314 loading solvent (Fig. 5a) since the solution had lower release percentage (< 0.02%)  
11  
12 315 and better solubility than methanol and methanol-water (90:10, v/v).  
13  
14  
15

### 16 316 **3.4.3. Screening of washing solvent**

17  
18 317 The washing step is the most crucial point during SPE protocol since the  
19  
20 318 washing solvent must break non-specific interactions to discard matrix components.  
21  
22 319 In this investigation, 0.45 g of the MIPs was packed into home-made SPE column and  
23  
24 320 1 mg of the crude extracts was loaded onto the cartridge as described above. Several  
25  
26 321 solvents, different proportions of methanol-water (20:80, 30:70 and 40:60) (v/v), ethyl  
27  
28 322 acetate and acetone, were adopted respectively as possible acceptor solvents to wash  
29  
30 323 the imprinted polymer from 1 to 6 ml. The mixture of methanol-water (20:80 or 40:60,  
31  
32 324 v/v) led to increased ISO binding to the MIP than others (Fig. 5b). In view of the  
33  
34 325 complexity of real sample, the mixture of methanol-water (20:80, v/v) was considered  
35  
36 326 as the optimized washing solvent. It should be noted that the rinsing volume was  
37  
38 327 increased with the increasing of the amount of imprinted polymers used.  
39  
40  
41  
42  
43  
44  
45

### 46 328 **3.4.4. Evaluation of elution solvent**

47  
48 329 In present study, different volume of elution solvent, including acetonitrile and  
49  
50 330 acetonitrile-water mixture (10:90, 30:70, 50:50 and 60:40) (v/v), was explored to  
51  
52 331 choose the optimal elution solvent. As showing in Fig. 5c, the template molecule can  
53  
54 332 not be eluted out by 6 ml of acetonitrile and acetonitrile-water (10:90, v/v) while  
55  
56  
57  
58  
59  
60

1  
2  
3  
4 333 50:50 or 60:40 (v/v) of acetonitrile-water led to all the components eluted together  
5  
6 334 from the MIP. For the extract of cotton flower, good extraction efficiency was  
7  
8  
9 335 achieved by using acetonitrile-water (30:70, v/v) since the mixture seriously disturbs  
10  
11 336 the interaction of monomer to template with predominant hydrophobic effects.<sup>31</sup>

#### 12 13 14 337 **3.4.5 Effect of the amount of MIP in SPE**

15  
16 338 To evaluate the extraction efficiency, the proposed MISPE method was applied  
17  
18 339 to a diluted extract of cotton flower which mainly contains flavonoids. After  
19  
20 340 optimization of the MISPE protocols, methanol-water (70:30, v/v) of 0.5 ml was used  
21  
22 341 as loading solvent, methanol-water (20:80, v/v) of 5 ml and methanol-water (25:75,  
23  
24 342 v/v) of 5 ml was used as washing solvent, respectively, and acetonitrile-water (30:70,  
25  
26 343 v/v) was adopted as elution solvent. Different amounts of MIPs, i.e., 0.45 g, 0.9 g and  
27  
28 344 1.9 g, were packed into home-made SPE column then for the specific extraction of  
29  
30 345 ISO from the crude extracts and segmented gather the sample by TLC. As expected,  
31  
32 346 an increase in amount of MIP led to an increase in the bound amount of the template  
33  
34 347 and its analogues (Table S2). 0.9-MIPs (0.9 g) was the optimum rather than  
35  
36 348 0.45-MIPs and 1.9-MIPs in a compromise of the recovery rate of ingredients and  
37  
38 349 extraction time. The huge peaks from the crude extract of cotton flower were  
39  
40 350 eliminated and very little other unwanted peaks were seen in the rest of the  
41  
42 351 chromatograms (Fig. 6). Different from the results with conventional silica-based  
43  
44 352 material as SPE, the retention time of AST is smaller than ISO and HYP. This may be  
45  
46 353 due to the lacking of hydroxyl in 3'-position of aglycone on the molecular structure of  
47  
48  
49  
50  
51  
52  
53  
54  
55  
56  
57  
58  
59  
60

1  
2  
3  
4 354 AST. The highest recovery rate of ISO, HYP and AST was 87.93%, 93.00% and  
5  
6 355 83.25%, respectively (Table 3).  
7

#### 8 356 **4. Conclusion**

9  
10  
11 357 The ISO-MIP was successfully achieved with ionic liquid as the composition  
12  
13 358 porogenic solvent. The selectivity of the ISO-MIP against the structure-related  
14  
15 359 flavonoid glycosides was also demonstrated. In addition, the optimization of MISPE  
16  
17 360 procedure, the amount of imprinting polymer, loading step, washing step and elution  
18  
19 361 step, has been explored. Then the SPE based on ISO-MIP was allowed to purify  
20  
21 362 specifically flavonoid glycosides from the extract of cotton flower with the high  
22  
23 363 recoveries for isoquercitrin, hyperoside, and astragalin. As a conclusion, the approach  
24  
25 364 provided a new method for the separation and preconcentration of ISO and its analogs  
26  
27 365 from natural products. Future work will be undertaken to improve the purity of  
28  
29 366 isoquercitrin and its analogues of the MISPE method.  
30  
31  
32  
33  
34

#### 35 367 **Acknowledgments**

36  
37  
38 368 This work was financially supported by the High Technology Research and  
39  
40  
41 369 Development Program of Xinjiang (No. 201217149).  
42  
43  
44  
45  
46  
47  
48  
49  
50  
51  
52  
53  
54  
55  
56  
57  
58  
59  
60

370 **References**

- 371 1 S. Itagaki, S. Oikawa, J. Ogura, M. Kobayashi, T. Hirano, and K. Iseki, *Food*  
372 *Chem.*, 2010, **118**, 426.
- 373 2 I. B. Afanas'eva, E. A. Ostrakhovitch, E. V. Mikhal'chik, G. A. Ibragimova, and L.  
374 G. Korkina, *Biochem. Pharmacol.*, 2001, **61**, 677.
- 375 3 P. Marimuthu, C. L. Wu, H. T. Chang, and S. T. Chang, *J. Sci. Food Agric.*, 2008,  
376 **88**, 1400.
- 377 4 K. Hartonen, J. Parshintsev, K. Sandberg, E. Bergelin, L. Nisula, and M. Riekkola,  
378 *Talanta*, 2007, **74**, 32.
- 379 5 E. V. Petersson, J. Liu, P. J. R. Sjoberg, R. Danielsson, and C. Turner, *Anal. Chim.*  
380 *Acta*, 2010, **663**, 27.
- 381 6 F. C. Stenger, V. Cechinel-Filho, C. Meyre-Silva, T. M . B., Bresolin, and A. C.  
382 Rodrigues, *Chromatographia*, 2009, **69**, S183.
- 383 7 A. Kumar, A. K. Malik, and D. K. Tewary, *Anal. Chim. Acta*, 2009, **631**, 177.
- 384 8 F. Fang, J.-M. Li, Q.-H. Pan, and W.-D. Huang, *Food Chem.*, 2007, **101**, 428.
- 385 9 S.-P. Wang, and K.-J. Huang, *J. Chromatogr. A*, 2004, **1032**, 273.
- 386 10 P. Valentão, P. B. Andrade, F. Areias, F. Ferreres, and R. M. Seabra, *J. Agric.*  
387 *Food Chem.*, 1999, **47**, 4579.
- 388 11 P. Dugo, M. Lo Presti, M. Öhman, A. Fazio, G. Dugo, and L. Mondello, *J. Sep.*  
389 *Sci.*, 2005, **28**, 1149.
- 390 12 P. Mattila, J. Astola, and J. Kumpulainen, *J. Agric. Food Chem.*, 2000, **48**, 5834.
- 391 13 J. Pan, C. Zhang, Z. Zhang, and G. Li, *Anal. Chim. Acta*, 2014, **815**, 1.

- 1  
2  
3  
4 392 14 M. Lasáková, and P. Jandera, *J. Sep. Sci.*, 2009, **32**, 799.  
5  
6 393 15 V. Pichon, *J. Chromatogr. A*, 2007, **1152**, 41.  
7  
8  
9 394 16 F. G. Tamayo, E. Turiel, and A. Martín-Esteban, *J. Chromatogr. A*, 2007, **1152**,  
10  
11 395 32.  
12  
13 396 17 A. Pardo, L. Mespouille, B. Blankert, P. Trouillas, M. Surin, P. Dubois, and P.  
14  
15 397 Duez, *J. Chromatogr. A*, 2014, **1364**, 128.  
16  
17  
18 398 18 V. Pakade, E. Cukrowska, S. Lindahl, C. Turner, and L. Chimuka, *J. Sep. Sci.*,  
19  
20 399 2013, **36**, 548.  
21  
22 400 19 V. Pakade, S. Lindahl, L. Chimuka, and C. Turner, *J. Chromatogr. A*, 2012, **1230**,  
23  
24 401 15.  
25  
26  
27 402 20 J. O'Mahony, A. Molinelli, K. Nolan, M. R. Smyth, and B. Mizaikoff, *Biosens.*  
28  
29 403 *Bioelectron.*, 2006, **21**, 1383.  
30  
31  
32 404 21 J. Xie, L. Zhu, H. Luo, L. Zhou, C. Li, and X. Xu, *J. Chromatogr. A*, 2001, **934**, 1.  
33  
34  
35 405 22 K. Booker, M. C. Bowyer, C. I. Holdsworth, and A. McCluskey, *Chem. Commun.*,  
36  
37 406 2006, **11**, 1730.  
38  
39 407 23 K. Booker, C. I. Holdsworth, C. M. Doherty, A. J. Hill, M C. Bowyer and A.  
40  
41 408 McCluskey, *Org. Biomol. Chem.*, 2014, **12**, 7201.  
42  
43 409 24 D. D. Zhong, Y. P. Huang, X. L. Xin, Z. S. Liu, and H. A. Aisa, *J. Chromatogr. B*,  
44  
45 410 2013, **934**, 109.  
46  
47  
48 411 25 L. H. Bai, X. X. Chen, Y. P. Huang, Q. W. Zhang, and Z. S. Liu, *Anal. Bioanal.*  
49  
50 412 *Chem.*, 2013, **405**, 8935.  
51  
52  
53 413 26 H.-F. Wang, Y.-Z. Zhu, X.-P. Yan, R.-Y. Gao and J.-Y. Zheng, *Adv. Mater.*, 2006, **18**,  
54  
55  
56  
57  
58  
59  
60

- 1  
2  
3  
4 414 3266.  
5  
6 415 27 G. Wulff, *Angew. Chem. Int. Ed.*, 1995, **34**, 1812.  
7  
8  
9 416 28 G. Wulff, *Chem. Rev.*, 2002, **102**, 1.  
10  
11 417 29 L. Zhao, L. Ban, Q. W. Zhang, Y. P. Huang, and Z.S. Liu, *J. Chromatogr. A*, 2011,  
12  
13 418 **1218**, 9071.  
14  
15  
16 419 30 S. E. Holroyd, P. Groves, M. S. Searle, U. Gerhard, and D. H. Williams,  
17  
18 420 *Tetrahedron*, 1993, **49**, 9171.  
19  
20  
21 421 31 S. K. Tsermentselia, P. Manesiotisb, A. N. Assimopouloua, V. P. Papageorgiou, *J.*  
22  
23 422 *Chromatogr. A*, 2013, **1315**, 15.  
24  
25  
26 423  
27  
28  
29  
30  
31  
32  
33  
34  
35  
36  
37  
38  
39  
40  
41  
42  
43  
44  
45  
46  
47  
48  
49  
50  
51  
52  
53  
54  
55  
56  
57  
58  
59  
60

1  
2  
3  
4 424 **Legends**  
5

6 425 **Fig. 1.** Structures of ISO and its analogues tested. (a) ISO, (b) HYP, (c) AST.  
7

8 426 **Fig. 2.** Morphologies characterization of ISO-imprinted polymer (P15) determined by  
9  
10 (a) SEM (b) mercury intrusion porosimetry.  
11

12 428 **Fig. 3.** Van't Hoff plots by plotting  $\ln k'$  vs.  $1/T$  (a) and  $\ln a$  vs.  $1/T$  (b) on imprinted  
13  
14 monolith (P15). Mobile phase: methanol/water/acetate acid (90/9/1, v/v/v); detection  
15  
16 wave length: 255 nm; flow rate: 0.5 mL/min; injection: 20  $\mu$ L; temperature: 25-45°C.  
17  
18  
19 430

20 431 **Fig. 4.** Selectivity of ISO imprinted monolith (P15). Mobile phase,  
21  
22 methanol/water/acetate acid (90/9/1, v/v/v); velocity of flow, 0.5 ml/min; detection  
23  
24 wavelength, 255 nm; injection volume, 20  $\mu$ l; temperature: 30°C.  
25  
26  
27 433

28 434 **Fig. 5** Optimization of the MISPE procedure. Screening of the appropriate (a) loading  
29  
30 solvent, (b) washing solvent, (c) elution solvent.  
31  
32

33 436 **Fig. 6** Chromatograms of the crude extracts before the MISPE column, after the  
34  
35 MISPE column and the eluent from MISPE. (a) HYP, (b) ISO, (c) AST. The mobile  
36  
37 phase consisted of solvent A (method) and solvent B (3% phosphoric acid aqueous  
38  
39 solution) and solvent D (acetonitrile) with following gradient: 12% A, 77% B, 11% D,  
40  
41 439 0→28 min; 12% A, 77→66% B, 11→22% D, 28→60 min; 12% A, 66→65% B,  
42  
43 440 22→23% D, 60→90 min. Flow rate, 0.5 ml/min; detection wavelength, 255 nm;  
44  
45 441 injection volume, 20  $\mu$ l; temperature 30°C.  
46  
47 442  
48  
49  
50 443  
51  
52  
53  
54  
55  
56  
57  
58  
59  
60

444

445 **Table 1** Preparation protocol for MIP monoliths.

Column NO.	ISO (mg)	4-VP ( $\mu$ L)	AM (mg)	MAA ( $\mu$ L)	DMF (mL)	EDMA ( $\mu$ L)	DMSO (mL)	[BMIM]BF <sub>4</sub> (mL)	AIBN (mg)	T ( $^{\circ}$ C)	IF
1	209.0	192	--	--	0.24	1359	1.2	2.468	20	60	2.085
2	--	192	--	--	0.24	1359	1.2	2.468	20	60	--
3	167.2	192	--	--	0.24	1359	1.2	2.468	20	60	2.347
4	--	192	--	--	0.24	1359	1.2	2.468	20	60	--
5	139.3	192	--	--	0.24	1359	1.2	2.468	20	60	2.277
6	--	192	--	--	0.24	1359	1.2	2.468	20	60	--
7	167.2	192	--	--	0.24	1019	1.2	2.468	20	60	1.623
8	--	192	--	--	0.24	1019	1.2	2.468	20	60	--
9	167.2	192	--	--	0.24	1699	1.2	2.468	20	60	1.327
10	--	192	--	--	0.24	1699	1.2	2.468	20	60	--
11	167.2	--	127.9	--	0.24	1359	1.2	2.468	20	60	0.967
12	--	--	127.9	--	0.24	1359	1.2	2.468	20	60	--
13	167.2	--	--	514	0.24	1359	1.2	2.468	20	60	0.976
14	--	--	--	514	0.24	1359	1.2	2.468	20	60	--
15	167.2	192	--	--	0.12	1359	1.2	2.588	20	60	2.340
16	--	192	--	--	0.12	1359	1.2	2.588	20	60	--
17	167.2	192	--	--	0.48	1359	1.2	2.348	20	60	1.703
18	--	192	--	--	0.48	1359	1.2	2.348	20	60	--
19	167.2	192	--	--	0.06	1359	1.2	2.648	20	60	2.430
20	--	192	--	--	0.06	1359	1.2	2.648	20	60	--
21	167.2	192	--	--	--	1359	1.2	2.708	20	60	N.D.
22	--	--	--	--	--	1359	1.2	2.708	20	60	--

446

447

448

449

450

451

452

453

**Table 2** The thermodynamic parameters of molecularly imprinted column (P15)

Analytes	$\Delta H$ (kJ mol <sup>-1</sup> )	$\Delta S$ (Jmol <sup>-1</sup> K <sup>-1</sup> )	R	$\Delta\Delta H$ (kJmol <sup>-1</sup> )	$\Delta\Delta S$ (Jmol <sup>-1</sup> K <sup>-1</sup> )	R
ISO	-16.57	-47.67	0.999	--	--	--
methyl gallate	-12.82	-42.39	0.993	-3.75	-5.28	0.881
gallic acid	-12.75	-42.35	0.996	-3.82	-5.32	0.978
catechin	-15.11	-49.84	0.999	-1.46	-2.17	0.935
MHBA	-12.36	-47.56	0.999	-4.21	-0.11	0.980
PHBA	-13.29	-51.36	0.996	-3.28	-3.69	0.921

454

455

456

457

458

459 **Table 3** The IF value and retention parameters of ISO and it analogues on P15.

Entry	MIP monolith		NIP monolith		IF	Recovery rate (%)
	Retention time (min)	Retention factor	Retention time (min)	Retention factor		
isoquercitrin	10.866	3.03	5.445	1.02	2.97	61.26
hyperoside	9.805	2.63	5.645	1.09	2.41	74.75
astragalin	5.708	1.11	4.924	0.82	1.35	57.62
quercetin	32.59	10.88	18.60	5.37	2.02	N.D.
catechin	5.306	0.97	5.023	0.86	1.12	N.D.
MA	5.648	1.09	3.99	0.48	2.28	N.D.
GA	5.062	0.88	3.915	0.45	1.94	N.D.
MHBA	3.967	0.47	3.882	0.44	1.07	N.D.
PHBA	3.848	0.43	3.793	0.41	1.05	N.D.

460 N.D. not determined

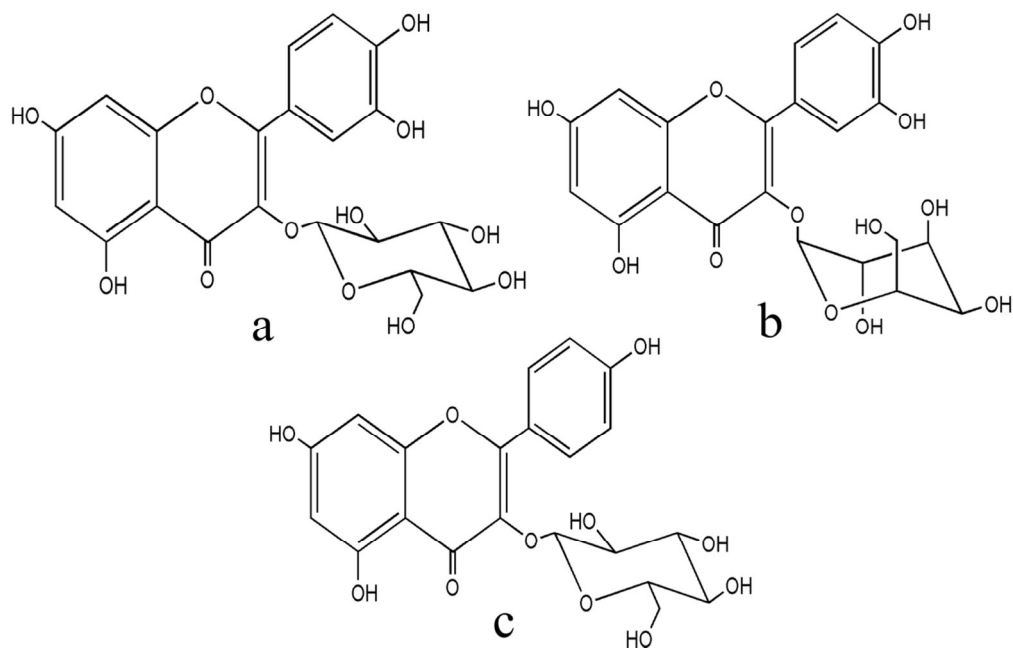


Fig. 1. Structures of ISO and its analogues tested. (a) ISO, (b) HYP, (c) C.  
52x33mm (600 x 600 DPI)

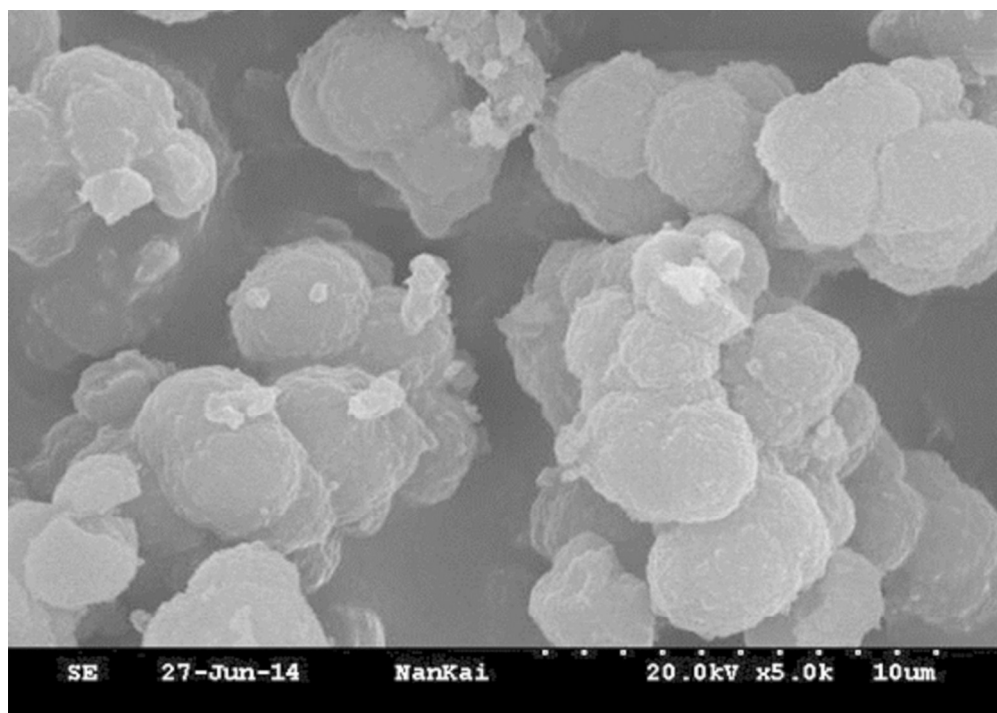


Fig. 2a. Morphologies characterization of ISO-imprinted polymer (P15) determined by SEM.  
82x58mm (300 x 300 DPI)

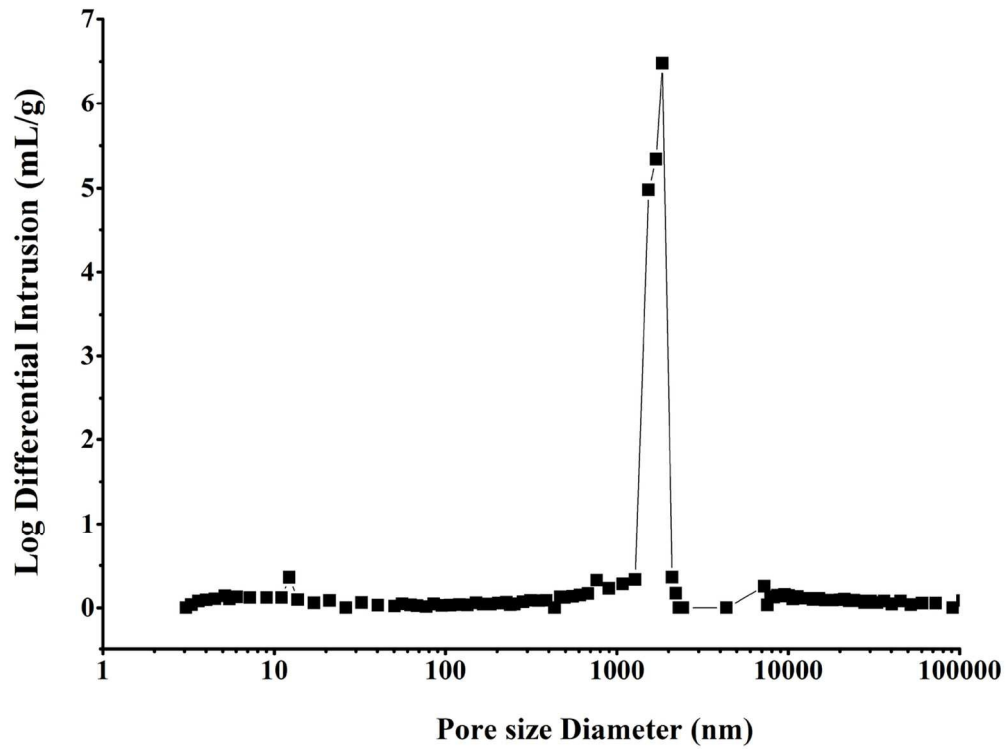


Fig. 2b. Morphologies characterization of ISO-imprinted polymer (P15) determined by mercury intrusion porosimetry.  
61x46mm (600 x 600 DPI)

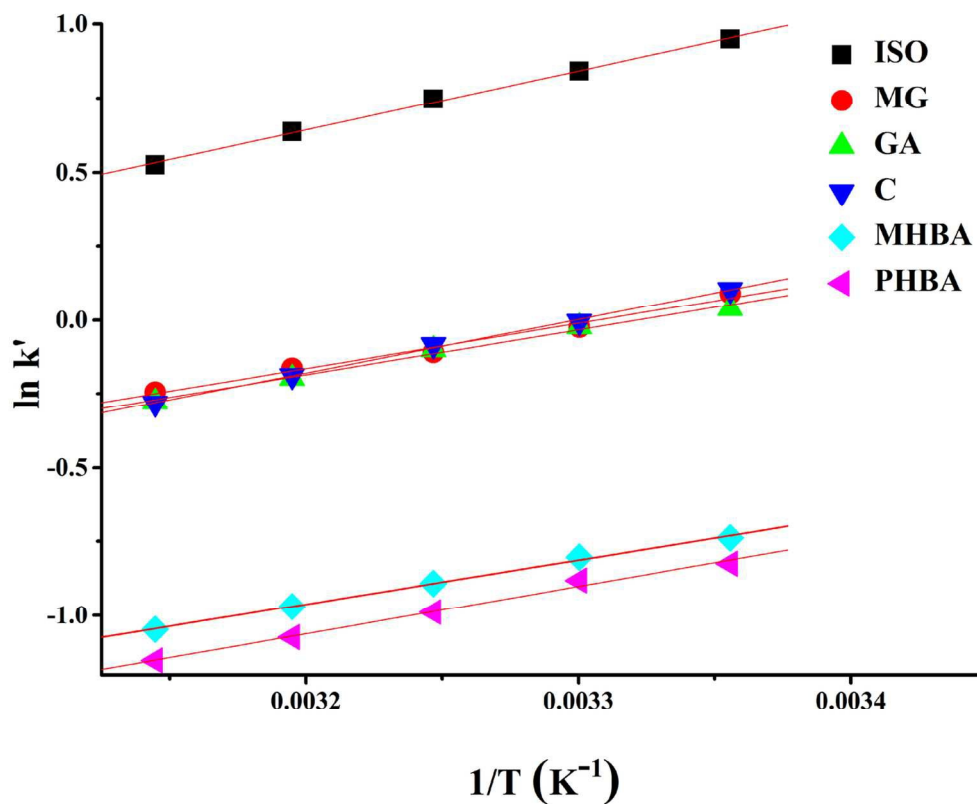


Fig. 3a. Van't Hoff plots by plotting  $\ln k'$  vs.  $1/T$  (a) on imprinted monolith (P15). Mobile phase: methanol/water/acetate acid (90/9/1, v/v/v); detection wave length: 255 nm; flow rate: 0.5 mL/min; injection: 20  $\mu$ L; temperature: 25-45°C.  
61x49mm (600 x 600 DPI)

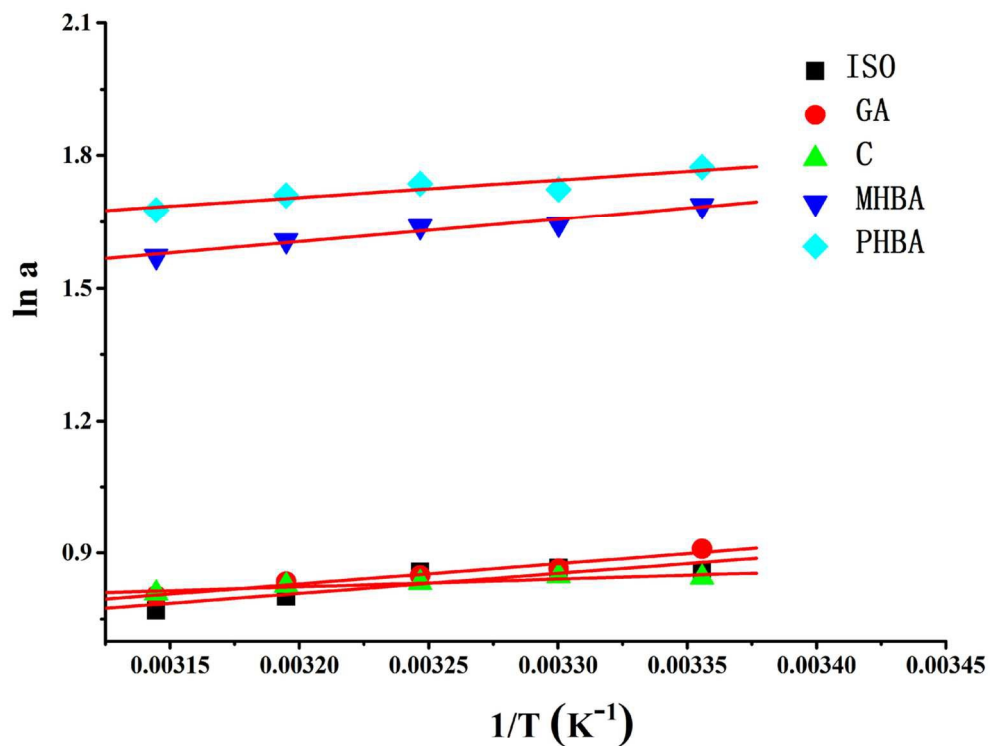


Fig. 3b. Van't Hoff plots by plotting  $\ln a$  vs.  $1/T$  on imprinted monolith (P15). Mobile phase: methanol/water/acetate acid (90/9/1, v/v/v); detection wave length: 255 nm; flow rate: 0.5 mL/min; injection: 20  $\mu$ L; temperature: 25-45°C.  
56x42mm (600 x 600 DPI)

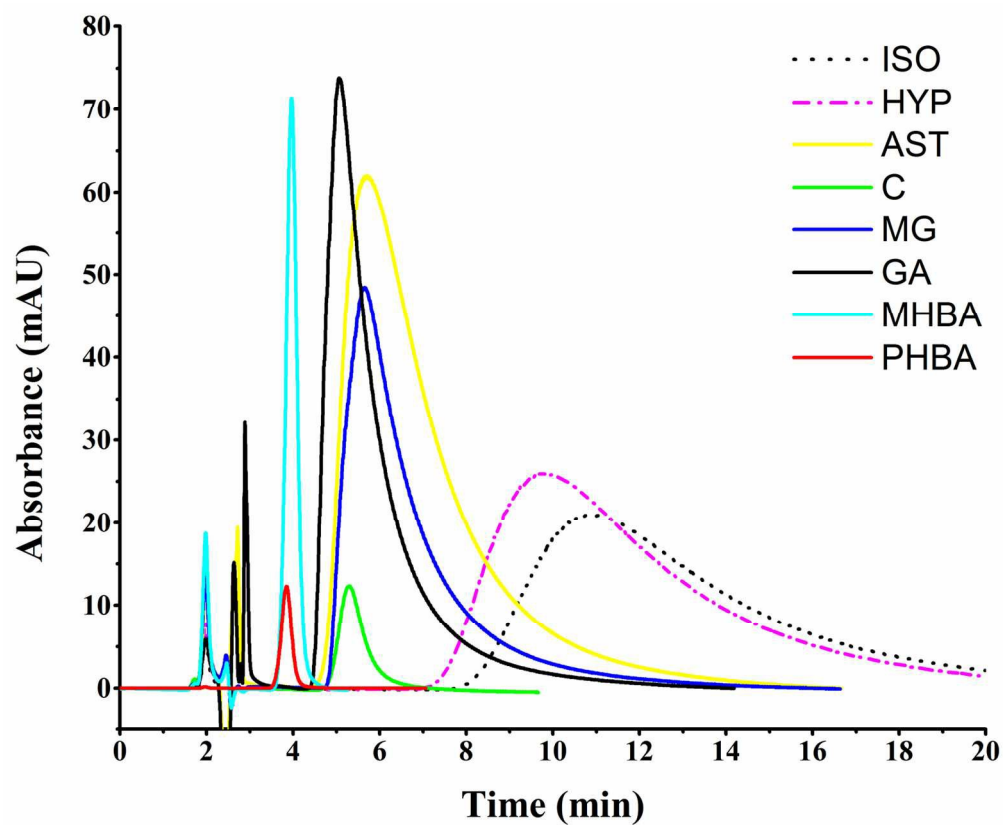


Fig. 4. Selectivity of ISO imprinted monolith (P15). Mobile phase, methanol/water/acetate acid (90/9/1, v/v/v); velocity of flow, 0.5 ml/min; detection wavelength, 255 nm; injection volume, 20  $\mu$ l; temperature: 30°C.  
69x57mm (600 x 600 DPI)

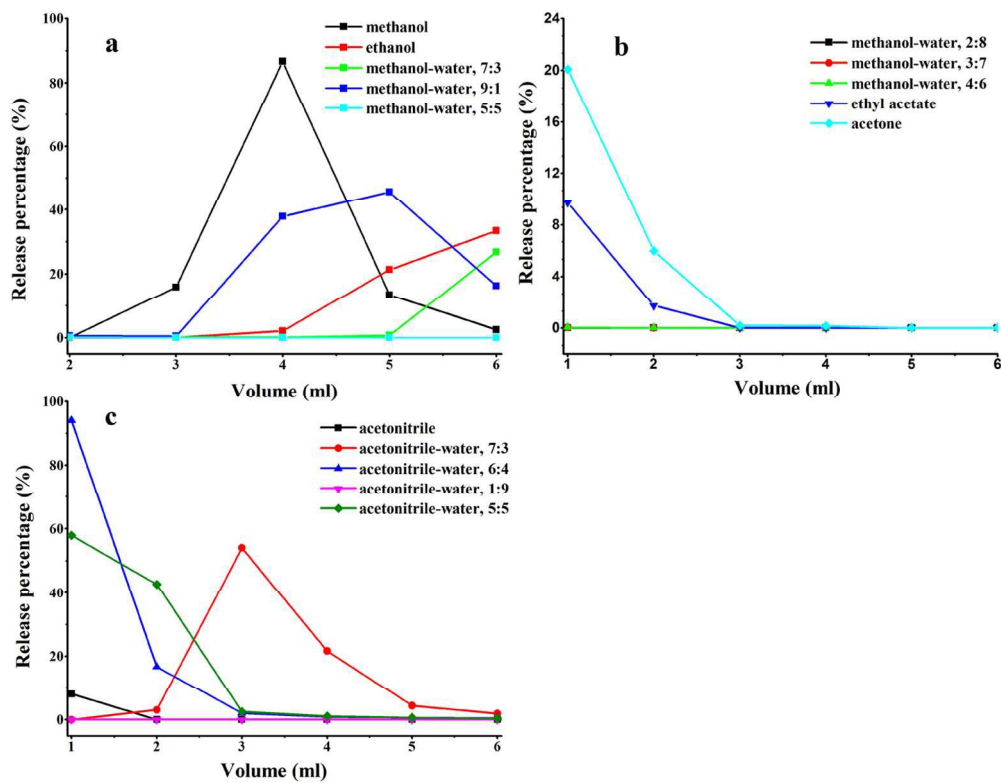


Fig. 5 Optimization of the MISPE procedure. Screening of the appropriate (a) loading solvent, (b) washing solvent, (c) elution solvent.  
64x50mm (600 x 600 DPI)

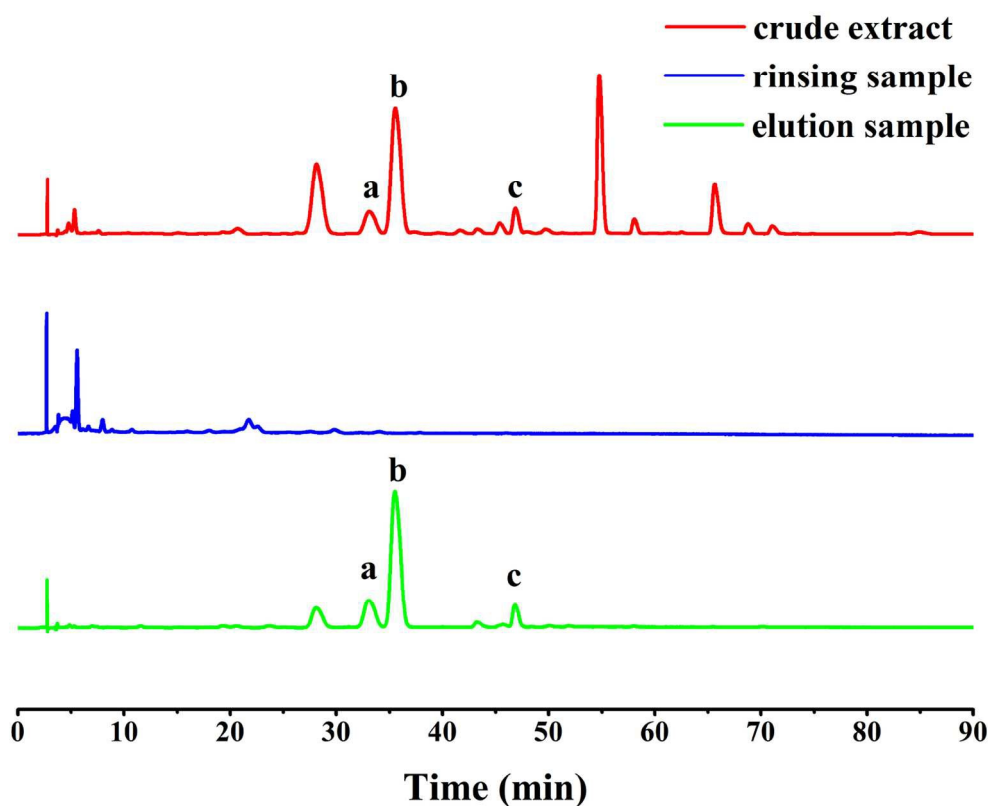


Fig. 6 Chromatograms of the crude extracts before the MISPE column, after the MISPE column and the eluent from MISPE. (a) HYP, (b) ISO, (c) AST. The mobile phase consisted of solvent A (method) and solvent B (3‰ phosphoric acid aqueous solution) and solvent D (acetonitrile) with following gradient: 12% A, 77% B, 11% D, 0→28 min; 12% A, 77→66% B, 11→22% D, 28→60 min; 12% A, 66→65% B, 22→23% D, 60→90 min. Flow rate, 0.5 ml/min; detection wavelength, 255 nm; injection volume, 20  $\mu$ l; temperature 30°C.

69x58mm (600 x 600 DPI)